

An Optically Controlled Isolator using Ferrite Edge Mode

Toshiro Kodera

Osaka Institute of Technology, Osaka, 535-8585, Japan

Abstract — This paper introduces a new type of microwave isolator. The nonreciprocity of the isolator can be optically controlled. The operation is based on the two phenomena: the ferrite edge-mode and the photo-generated plasma on silicon substrate. Conventional ferrite edge-mode isolator has been made of the ferrite and the resistive material. The later is used to absorb the reverse-propagating wave of the isolator. An inadequate choice of the resistive body leads to the imperfect absorption; the isolation ratio decreases. In this paper, a novel isolator is introduced by using this change of isolation. The optical control is realized by changing the intensity of illumination to produce the variety of the plasma density on the silicon substrate. On the isolator, the frequency response is investigated both experimentally and numerically. The numerical analysis is performed by the FDTD method. Both numerical and experimental results have shown that the isolation ratio can be controlled for 39dB at 11GHz by the laser-illumination on the silicon substrate.

I. INTRODUCTION

In many microwave systems, the nonreciprocal devices using ferrite media are widely used from a viewpoint of stabilization and protection. The most fundamental parameter that determines the operation of ferrite devices is the applied dc magnetic field. Changing the intensity of this field can control the characteristic of the device. However, the spiral coil to produce the variable magnetic field imposes the problems of size, drive speed, and drive current.

On the other hand, it is well known that the solid-state plasma on the semiconductor induced by illumination can broadly change the surface resistance [1]. In this paper, the photoconductive effect of the silicon and the ferrite edge mode are combined to realize the optically controlled isolator. The isolator achieves the change of characteristics without a lot of problems inherit in the magnetic control.

II. PRINCIPLE OF OPERATION

First, the basic principle of the isolator is explained. As shown in fig.1, the field distribution of the ferrite edge mode is concentrated on the left-hand side under the metal strip regarding to the propagation direction provided that the dc magnetic field is applied upward to

the substrate[2]. In order to consider the basic operation of the isolator presented here, the influence of the resistive material loaded on the one side of the strip edge on the transmission characteristic is considered on the isolator in fig.2.

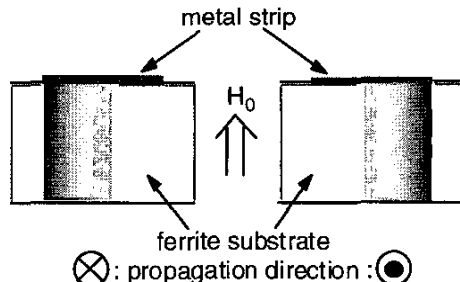


Fig.1 field distribution of the ferrite edge mode.

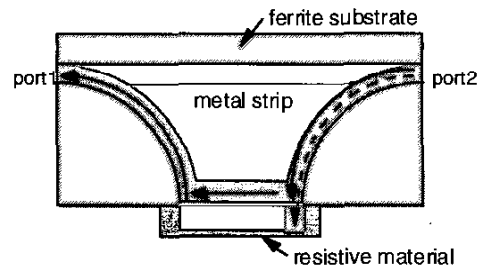


Fig.2 Changes of transmission state as a response to the conductivity. In case of the matching condition satisfied, input signal is terminated at the resistive material, otherwise reflected at the edge of the stripline with ferrite substrate.

Figure 2 shows a model of the conventional ferrite edge-mode isolator. The model consists of three parts including ferrite substrate, resistive material, and metal strip. In case of the propagation from port1 to port2, that is the forward transmission; the propagation is performed without the influence of the resistive material owing to the nature of the mode in fig.1. Next, the reverse-transmission is considered. At the connection point between ferrite and resistive material, when the equivalent impedance of striplines with ferrite and resistive material are equal, the input is terminated at the resistive material and no reflection will occur. This is the

cutoff state of the isolator, depicted in the dotted line of fig.2.

On the other hand, the impedance mismatch on the junction point between striplines with ferrite and silicon substrates bring about reflection, it leads to a transmission from port2 to 1. As a result, the nonreciprocity disappears. This is the through state of the isolator, which is shown in the solid lines of fig.2. In this way, the transmission can be controlled by the conductivity of the resistive material in the isolator.

Here, let us consider exchanging the resistive material for the silicon with photo-generated plasma. The relative permittivity of the photo plasma is given by (1) [1].

$$\epsilon_p = \epsilon_s - \sum_{i=e,h} \frac{\omega_{pi}^2}{\omega^2 + \gamma_i^2} \left(1 + j \frac{\gamma_i}{\omega} \right) \quad (1)$$

In (1), ω is angular frequency of the electromagnetic wave, and γ_i is collision frequency of the electron and hole, ω_{pi} is plasma angular frequency written in (2).

$$\omega_{pi} = \frac{n_i e^2}{\epsilon_0 m_i^*} \quad (i = e, h) \quad (2)$$

In (2), ϵ_0 is the permittivity in the vacuum, m_i^* is effective mass of electron and hole. n_i are the carrier density of electron and hole. In this paper, the carrier densities are chosen as the same as the plasma densities n_p in order to assume the intrinsic semiconductor. Here, material parameters of the high-resistivity silicon required in the calculation are summarized in table 1.

Table1 Material parameters for high-resistivity silicon.

relative permittivity of Si	$\epsilon_s = 11.8$
electronic charge	$e = 1.6 \times 10^{-19} [C]$
effective mass of electrons	$m_e^* = 2.36 \times 10^{-31} [kg]$
effective mass of holes	$m_h^* = 3.46 \times 10^{-31} [kg]$
collision frequency of electrons	$\gamma_e = 4.50 \times 10^{12} [1/sec]$
collision frequency of holes	$\gamma_h = 7.71 \times 10^{12} [1/sec]$

The relative permittivity and conductivity for 9.5GHz can be derived from (1) as a function of the plasma density n_p .

$$\epsilon_{p_real} = 11.8 - 7.41 \times 10^{-22} n_p \quad (3)$$

$$\sigma = -\omega \epsilon_0 \epsilon_{p_img} = 3.39 \times 10^{-20} n_p \quad (4)$$

As given in eq.(3) and (4), in case of the operation frequency is enough low compared to the collision frequency of electron and hole, the change of the dielectric constant turns into about 1% of the change of the conductivity. Based on this characteristic of plasma,

the numerical model of the plasma-induced silicon is established by neglecting the change of the permittivity.

III. NUMERICAL MODELING

Figure 3 shows the geometry of the numerical model in this paper. The numerical computation is conducted by the FDTD method with the extension to provide the gyromagnetic property of the ferrite media. The formulation scheme of ferrite media is described in [3].

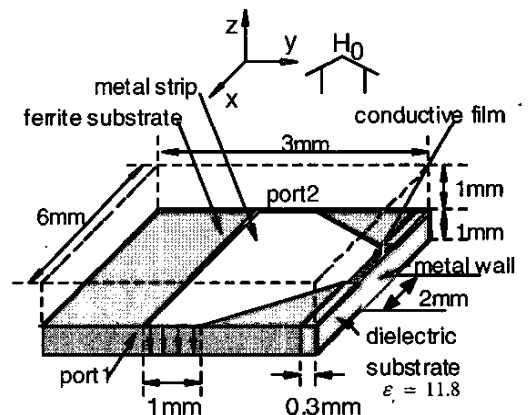


Fig.3 Schematic of the analytical model.

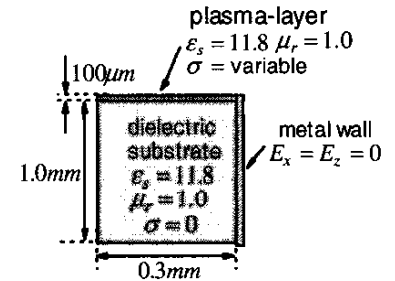


Fig.4 Analytical model of the plasma-induced silicon.

Figure 4 shows the numerical model of plasma-induced silicon. The model consists of two parts including dielectric and conductive material. Each region corresponds to the silicon substrate and the plasma layer. The right side of the model in fig.4 is assumed to be a metal wall. The relative dielectric constant of both regions is set up to 11.8. The analysis is carried out with the change of the conductivity of the plasma layer. The thickness of the plasma layer is decided by using the following equation of the diffusion length [1].

$$L_D = \sqrt{\frac{2\mu_e \mu_h}{\mu_e + \mu_h} \frac{k_B T}{e} \tau} \quad (5)$$

In this equation, μ_e and μ_h are the mobility of electron and hole. k_B is the Boltzmann constant, and τ is the lifetime of electron-hole pair. The diffusion length of plasma, L_D for $T=300K$, $\tau=10\mu s$ can be calculated as $150\mu m$. The thickness of the plasma layer, namely the thickness of the conductive layer is set up to $100\mu m$,

Table 2 Parameters for the numerical analysis

applied dc magnetic field	0.21T
saturation magnetization of ferrite	0.18T
magnetic loss of ferrite ΔH	50 Oe
$dx = dy = dz$	0.1mm
Δt	0.17ps

which is same as the length of unit cell in FDTD analysis. The second order Mur's ABC is applied to the outside of the air region. The excitation is performed so that each Poynting vector direct to the opposite port in the analytical model. The parameters in the numerical analysis are summarized in table 2.

IV. NUMERICAL RESULTS

Figure 5 and 6 show the calculated transmission characteristics as a response to the conductivity of the plasma layer. From fig.5, it is found that the forward transmission S_{21} is not influenced by the value of conductivity at all. This result is provided by the nature of ferrite edge mode.

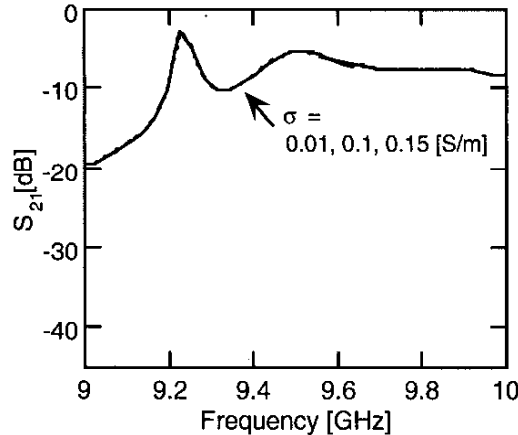


Fig.5 Numerical result of forward transmission S_{21} as a response to the conductivity.

Figure 6 shows the numerical result of reverse-transmission S_{12} as a response to the conductivity. Unlike the result of S_{21} in fig.5, it turns out that frequency response changes with the conductivity of plasma layer. According to the increase of the conductivity, the remarkable cutoff characteristics are brought about. The

maximum change of the isolation ratio, 30dB is obtained at the frequency of 9.57GHz. From the numerical results, it is cleared that the isolator has the feature that the isolation ratio can be changed in addition to the conventional nonreciprocity. The characteristic of the isolation ratio is confirmed to possess the peak characteristic which reaches the maximum value at $\sigma=0.15S/m$. These changes of the characteristics also have been confirmed by the changes of the field distribution.

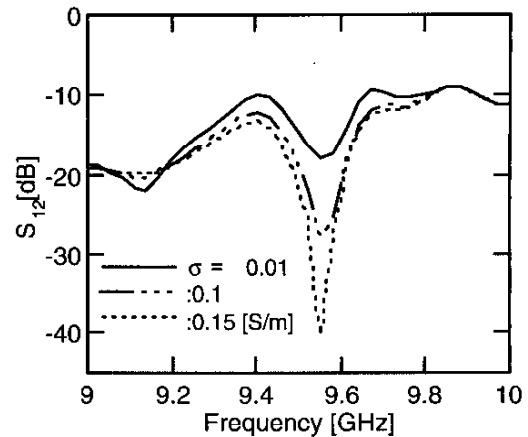


Fig.6 Numerical result of reverse transmission S_{12} as a response to the conductivity.

Judging from the numerical results shown above and the relationship between plasma density and conductivity, it is found that the reduction of conductivity without optical irradiation leads to break the matching condition: it turns into the transmission state. On the other hand, the increase of the conductivity by performing optical irradiation leads to the cutoff state with satisfying the matching condition at the edge. Based on the numerical results, the prototype isolator is fabricated experimentally.

V. EXPERIMENTAL RESULTS

Figure 7 shows the picture of the prototype isolator. The structure is explained by fig.8. The ferrite and silicon substrate is arranged on the ground plane. The strip line on the ferrite substrate is arranged by copper film. The ferrite material used here is the polycrystalline YIG of $5x5x1mm$. The saturation magnetization is $0.18T$, and the half value of magnetic resonance ΔH is $50Oe$. The dc magnetic field is applied by Nd-Fe-B permanent magnets with $10mm$ radius and $5mm$ thickness. The intensity of magnetic field at the ferrite surface is $0.38T$. The stripline with inter-digital structure on the silicon substrate is

formed by Au evaporation. The gap interval is set to 50 μ m as shown in fig.7. By applying this structure, it is confirmed that the cutoff characteristics of this isolator can be enhanced. The edge of silicon substrate is connected with the ground plane by the electro-conductive glue based on Ag. The gap portion is illuminated by the laser diode with wavelength of 830nm and maximum power of 30mW. Figure 9 and 10 show the experimental results. In these figures, P_L stands for the output power of the laser. The measurement is performed at $P_L=0$, 14.4, 24, 28, and 31mW.

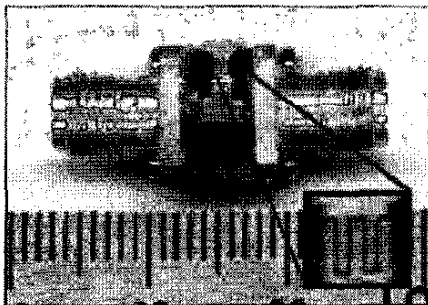


Fig.7 Picture of the prototype isolator.

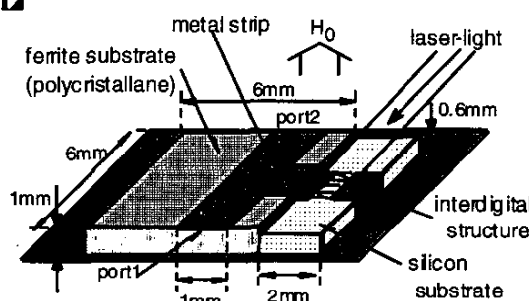


Fig.8 Schematic of the prototype isolator.

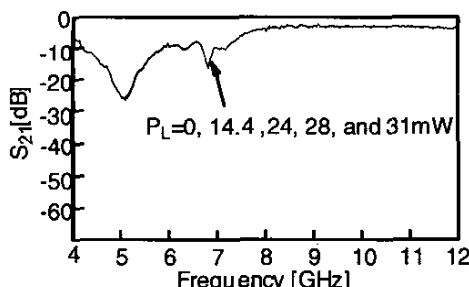


Fig.9 Experimental result of the forward transmission S_{21} .

Figure 9 shows the measurement result of S_{21} . The characteristic is not influenced by the intensity of the laser-illumination at all. This result is caused by the nature of the ferrite guide mode as investigated above.

The other, fig.10 shows the measurement result of reverse transmission. As shown, the cutoff property clearly appears according to the increase of the intensity of laser illumination. The tuning characteristics of this notch frequency by the applied dc magnetic field are also confirmed. The experimental results with the laser illumination by 31mW and null indicate that the control width of the isolation ratio is achieved as 39dB.

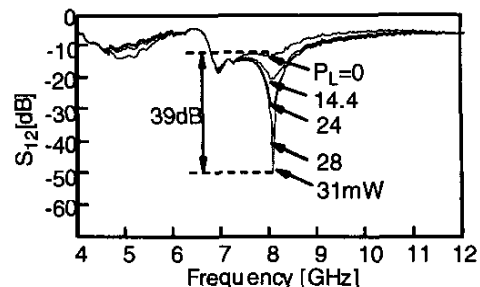


Fig.10 Experimental result of the reverse transmission S_{12} .

VI. CONCLUSION

In conclusion, proposal and verification are performed on the new type of isolator that combines the optical conduction effect of silicon and the magnetic characteristic of ferrite media. The prototype isolator introduced in this paper operates not only the optical controlled isolator but also the nonreciprocal microwave modulator by the light wave. The configuration should be useful for various microwave signal processing.

ACKNOWLEDGEMENT

The author would like to express his gratitude to Prof. Y. Satomura of Osaka Institute of Technology and Prof. M. Tsutsumi of Fukui University of Technology for constructive suggestions related to this work.

REFERENCES

- [1] M. Matsumoto, M. Tsutsumi and N. Kumagai : "Radiation of Millimeter Waves from a Leaky Dielectric Waveguide with a Light-Induced Grating Layer," IEEE Trans. MTT, MTT-35, No.11, pp.1033-1041, Nov. 1987.
- [2] M.E. Hines : "Reciprocal and Nonreciprocal Models of Propagation in Ferrite Stripline and Microstrip Devices," IEEE Trans. Microwave Theory and Tech., MTT-19, No.5, pp. 442-451, May 1971.
- [3] T. Kodera, H. Shimasaki, and M. Tsutsumi, "An analysis on magnetostatic waves by FDTD method," IEICE Trans. Electron., vol.E83-C, no.5, pp.713-719, May 2001.